CHANNEL MIGRATION MODEL FOR MEANDERING RIVERS

Timothy J. Randle, Supervisory Hydraulic Engineer,
U.S. Department of the Interior, Bureau of Reclamation,
Sedimentation and River Hydraulics Group
Denver, Colorado, trandle@do.usbr.gov

INTRODUCTION

The migration of river channels across their floodplains and the occasional erosion of terrace banks is a natural process (Leopold et al., 1964; Yang, 1971; Dunne and Leopold, 1978; Leopold, 1994; and Thorne, 1992 and 2002). This process becomes especially important to people living in or near the floodplain or to organizations planning or maintaining infrastructure within or along the edge of the floodplain. Natural rates of channel migration can be accelerated by human or natural disturbance. For example, the clearing of floodplain vegetation can accelerate the rate of channel migration. This paper provides a summary of a channel migration model for meandering rivers (Randle, 2004).

METHODOLOGY

Meandering river bends are observed in natural river channels, at all scales, and in all parts of the world (Leopold et al., 1964; Thorne, 1992; and Leopold, 1994). The channel migration model assumes that the river is able to adjust its channel alignment, slope, width, and depth between the non-erodible boundaries of the river valley. These adjustments occur so that the sediment transport capacity of the river channel matches the upstream sediment supply rate without deposition or erosion along the channel bed. The channel continually evolves because the upstream rates of water and sediment are continually changing.

Bank Erosion Rate: The model simulates channel migration by computing bank erosion as a function of the sediment transport capacity, the radius of channel curvature, and the bank material properties acting to resist the erosion including vegetation, large woody debris, cohesion, and armoring. The equation for bank erosion is based on dimensional analysis of the controlling variables and the use of empirical coefficients. Equation 1 is proposed to predict the rate of bank erosion and channel migration.

$$B_e = \left\{ \left[a_1 C_s \left(\frac{W_b}{R_c} \right) \right]_{at\ L} - \left[a_2 \left(r_\gamma \frac{r_d}{h_b} \right) + a_3 \left(LWD \frac{d_W}{D} \right) + a_4 (PI) + a_5 \left(d_c \frac{h_b}{D} \right) \right]_{\text{at } L + \text{Phase Lag}} \right\} a_6 V \qquad (1)$$

where B_e = rate of bank erosion [L/T],
C_s = bed-material sediment concentration [ppm]
W_b = bankfull channel width [L]
R_c = channel radius of curvature [L]
L = distance along the channel
Phase Lag = planform phase lag along the channel (see Figure1)
r_γ = fraction of bank area covered by vegetation roots [%]
r_d = vegetation root depth [L]

h_b = bank height [L]
LWD = fraction of bank area covered by trees or large woody debris [%]
d_W = average height of large woody debris jams [L]
D = hydraulic depth of the channel [L]
PI = plastic index
d_c = portion of bank sediment too coarse for incipient motion [%]
V = mean channel velocity [L/T]
a_1 and a_6 are empirical coefficients and a_2, $a3$, a_4, and a_5, are weighting factors

All the parameters on the right-hand side of Equation 1 produce dimensionless terms except for the average channel velocity, which provides dimensions for the bank erosion rate [L/T]. The first set of terms in Equation 1 [a_1, C_s, (W_b/R_c)] are computed at some distance L along the channel. The following terms of Equation 1 act to resist the bank erosion and are computed at a phase lag distance downstream from point L. The velocity term of Equation 1 (a_6 V) is computed at a distance L along the channel. The computed rate of bank erosion from Equation 1 is multiplied by a time step (Δt) and then applied to the channel at a distance equal to L + phase lag.

The equation coefficients a_1 and a_6 must be determined empirically through calibration. Coefficients a_2, a_3, a_4, and a_5 are used to weight the relative importance of the terms acting to resist bank and erosion and can be set so that the weighting is equal. Not all of these coefficients may be important for a particular river reach.

The root structure of riparian vegetation can add cohesive properties to the river bank and reduce the rates of bank erosion if the roots are at least as deep as the bank is high. Otherwise, the bank can become undercut by erosion underneath the vegetation roots, which may cause the top portion of the bank to collapse. Trees that fall into the river from an eroding bank can add large woody debris to the bank and channel. Large woody debris, present along the river bank, tends to increase the channel roughness, slow velocity, and also reduces the rates of bank erosion. However, the woody debris may be floated away if the flow depths are larger than the cumulative height of the large woody debris jam.

The presence of riparian vegetation can be expressed as the root density along the local bank area (r_γ). The effectiveness of these roots can be expressed as the ratio of the root length to the bank height (r_d /h_b). A ratio much less than unity would mean that the roots are not deep enough to prevent erosion at the bank toe from undercutting the vegetation. The presence of riparian forests and large woody debris along the eroding bank can be expressed as a percentage of the local bank area occupied by trees and large woody debris (LWD). The ability of large woody debris to remain along the river bank can be expressed as the average ratio of the height of large woody debris jams to the hydraulic depth of the river channel (d_W /D). A ratio much less than unity would indicate that the woody debris would be floated away.

The plasticity index (PI) is used to characterize the cohesive properties of the bank material. The percentage of bank sediment that is too coarse for incipient motion in the river channel (d_c) is used to characterize the ability of coarse bank material to armor the toe of an eroding river bank. The ratio of bank height to hydraulic depth (h_b/D) accounts for the greater mass of armoring

material when a river bank is higher than normal. For alluvial banks within the floodplain, this ratio is normally equal to unity, but the ratio can be significantly greater in the case of high terrace banks.

Planform Phase Lag: River meander bends induce secondary currents that increase the flow velocities and shear stresses along the outer bank and decrease them along the inner bank. Consequently, sediment erosion occurs along the outer bank and deposition occurs along the inner bank (Leopold et al., 1964; Thorne, 1992; and Leopold, 1994). The tendency to erode the outer bank and deposit sediment along the inner bank causes the channel to migrate laterally.

Typically, the maximum rate of bank erosion along the outer bank is located some phase-lag distance downstream of the meander bend apex, which causes the river channel to migrate both across the floodplain and downstream along the river valley (see Figure 1). If there were no phase lag, the meander bends would only migrate laterally across the floodplain and increase in amplitude. If the phase lag were equal to the channel distance along one-fourth of a meander wavelength, then the meander bends would only migrate downstream without any increase in amplitude.

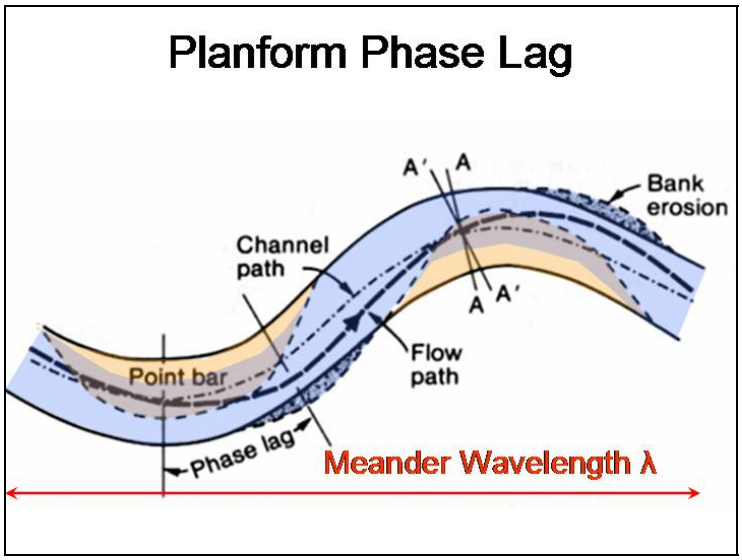

Figure 1 The greater the planform phase lag, the greater downstream migration of the meander bend along the valley axis.

In the model, the variable phase lag is determined by evaluating the river channel slope relative to the valley slope and the limiting channel slope associated with the minimum unit stream power. As the channel slope begins to approach the slope at the minimum unit stream power (*VS*), the migration of the meander bends will be primarily down valley. Since the channel slope is limited by both the valley slope and the slope at minimum *VS*, the planform phase lag should be proportional to the differences in these slopes (see Equation 2).

$$\text{Phase Lag} = \frac{\left(S_v - S_c\right)}{\left(S_v - S_{\min VS}\right)} C_{PL} \left(\frac{\Omega\ \lambda}{4}\right) \tag{2}$$

where S_v = valley slope
S_c = channel slope
$S_{\min VS}$ = channel slope at minimum VS
λ = meander wavelength
Ω = channel sinuosity
C_{PL} = a phase-lag coefficient, normally equal to 1.0

The model keeps track of the changing alignment throughout the simulation. At the beginning of each time step, the model computes the radius of curvature for each point along the channel alignment.

Model Input Requirements: The meander model input requirements include both initial conditions and boundary conditions. The initial conditions describe the river channel alignment and the material properties (vegetation, large woody debris, cohesion, and armor material) of the floodplain and terraces, including any lateral limits of channel migration. The boundary conditions describe the upstream inputs of water and sediment.

Initial Conditions The initial alignment of the river channel thalweg is digitally measured, in some Cartesian coordinate system, from rectified aerial photographs or from channel surveys. The river valley alignment and longitudinal slope are also measured from ortho-rectified aerial photography and topographic surveys. Channel cross-section data are not part of the model input. The model computes a channel width and depth for each time step and for each point along the channel alignment (Randle, 2004). The computation of cross section width and depth is based on the upstream inputs of water and sediment, Manning's equation for normal depth, a sediment transport capacity equation, and the minimum rate of energy dissipation theory (Yang and Song, 1979). However, the rate of change in channel width is limited to a certain percentage per time step.

Boundary Conditions The upstream boundary conditions include the discharge hydrograph and corresponding sediment supply. The model assumes that the upstream sediment supply is equal to the transport capacity for a specified cross section shape and channel slope.

Model Calibration and Validation: Measurements of historical channel migration should be used to calibrate and then validate the model results before the model is used for future predictions. The historic measurements of channel alignment could be divided into two independent time periods: one for model calibration and one for model validation.

EXAMPLE RESULTS

A 4.2-mile reach of the Hoh River, Washington was used to demonstrate the calibration and validation of the model. This reach is 5.5 miles downstream from the boundary of Olympic National Park and between river miles 21.4 and 25 (Piety et al., 2004). Historical aerial photographs of the Hoh River are available for the following years: 1950, 1960, 1971, 1977, 1981, 1994, 2001, and 2002. The initial channel alignment, for the model simulation, was digitized from the 1950 aerial photograph (see Figure 2).

The 27-year time period, from 1950 to 1977, was selected for model calibration. The 25-year time period, from 1977 to 2002, was selected for model validation. The 57-year record of mean-daily stream flow and annual peak flow is presented in Figure 3. Since there are no measurements of sediment load, the upstream sediment supply to the study reach was set equal to the sediment transport capacity (Randle, 2004).

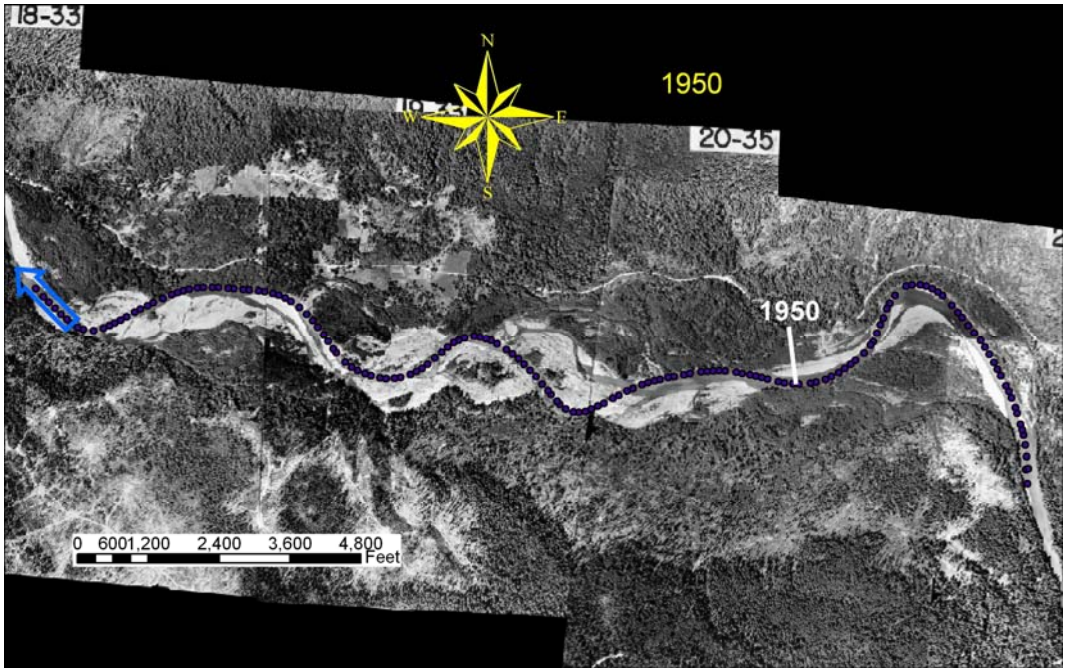

Figure 2 1950 aerial photograph and initial channel alignment.

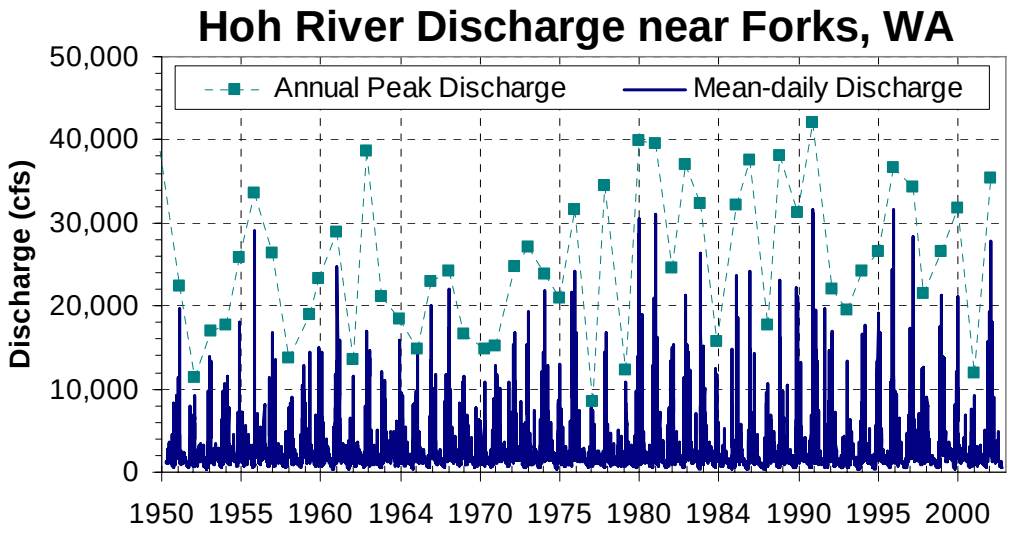

Figure 3 Mean-daily and annual-peak discharge of the Hoh River.

The bank material properties were globally defined for the modeled area and locally defined for seven smaller areas of the channel, floodplain, and terraces. The material properties for vegetation, large woody debris, cohesion, and armoring were determined for each area based on field inspection and were not subsequently adjusted during the calibration process.

Figure 4 shows a series of predicted channel alignments over the period 1950 to 2002. The model was not able to predict the meander-bend cutoff that occurred sometime between 1971 and 1977 (see Figure 5). Therefore, the predicted channel alignment was calibrated for the first two meander bends. The combination of coefficients a_1 and a_6 and the phase-lag coefficient that provided the best match between the predicted and measured channel alignments was determined by visual inspection of the model results compared to the 1977 aerial photographs.

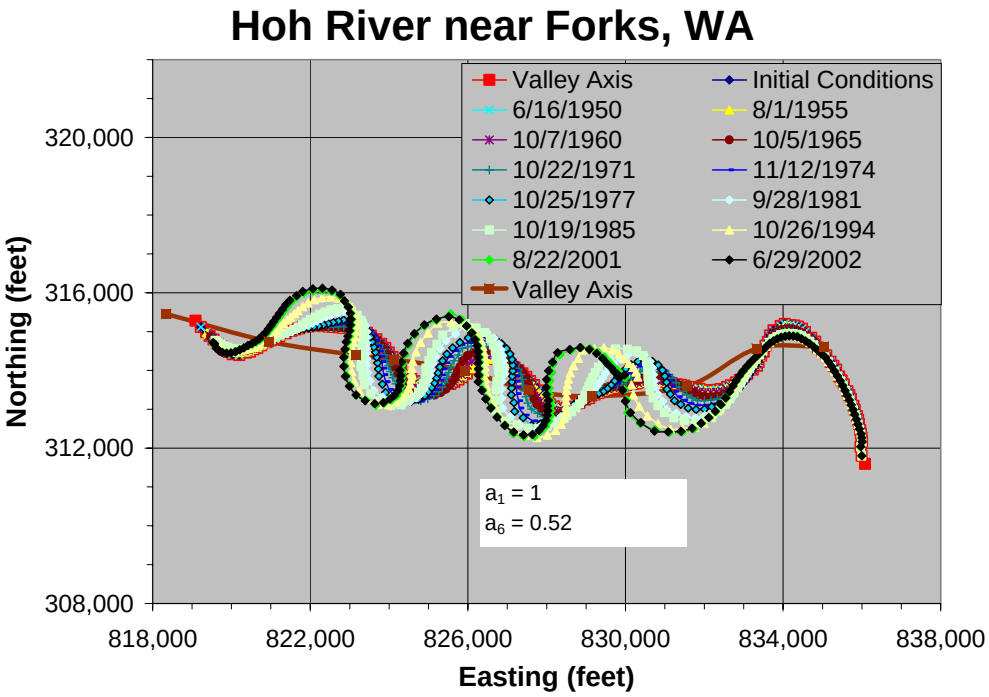

Figure 4 Predicted channel alignments for the period 1950 to 2002.

The model simulation was continued for the entire period (1950 to 2002). Although the model is not yet capable of predicting a meander-bend cutoff, the relatively short radius of curvature of the predicted meander bends would suggest that a cutoff is likely (see Figure 6).

DISCUSSION

Calibration was required for only two coefficients (a_1, a_6,) of Equation 1. The model was able to correctly predict the direction and approximate magnitude of channel migration for a least 10 years, until the cutoff of meander bends that first occurred between 1960 and 1971. Although the model is not yet able to predict the meander-bend cutoffs, they can be inferred from the tight radius of curvature from the predicted channel alignments.

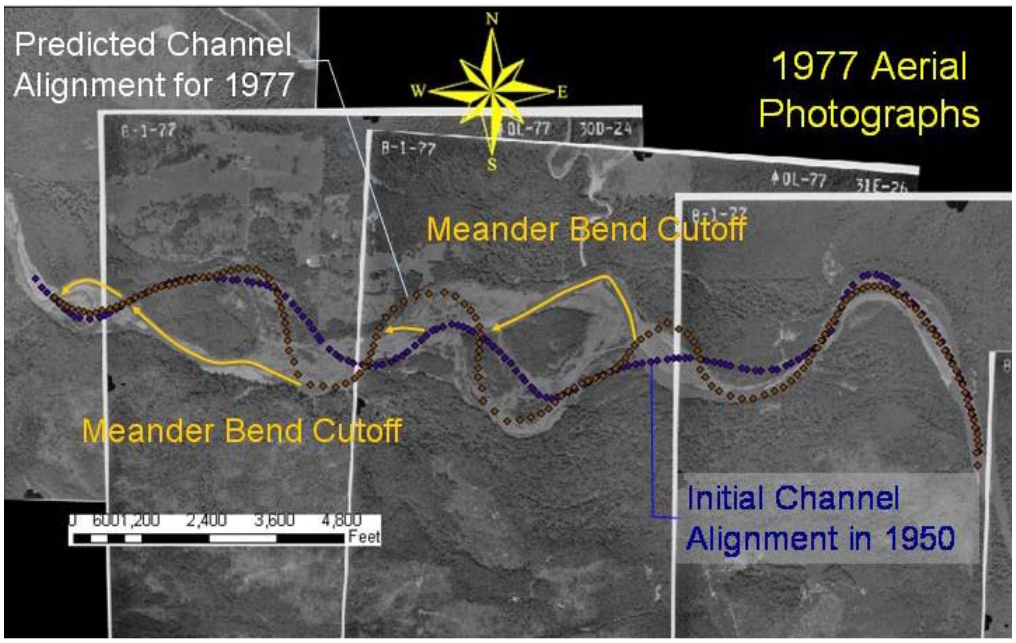

Figure 5 1977 aerial photograph and the initial (1950) and predicted (1977) channel alignments. A meander bend cutoff occurred sometime between 1971 and 1977.

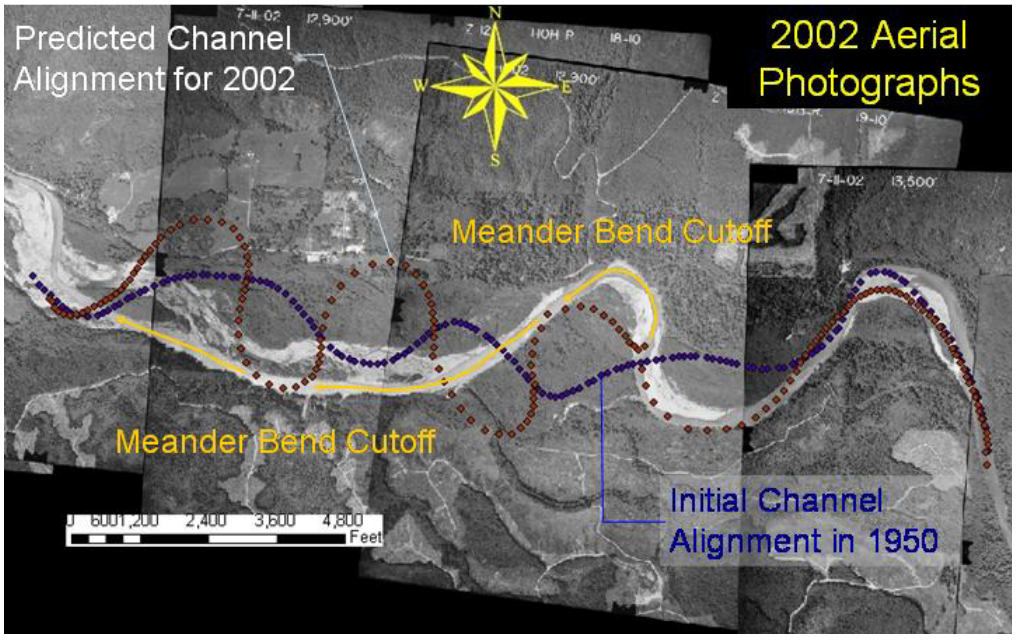

Figure 6 Initial (1950) and predicted (2002) channel alignments plotted on the 2002 aerial photograph.

The model correctly predicted that the initial direction of channel migration was in the lateral direction, across the floodplain. As the meander-bend amplitude increased, more of the meander-bend migration was in the down-valley direction (see Figure 4).

CONCLUSIONS

The channel migration model described in this paper does show promise as a tool for predicting future channel alignments. The model could be used to compare different hydrologic scenarios and alternative land use plans. The model could also be used to evaluate proposed highway and bridge alignments in the vicinity of the river channel and floodplain.

Additional research is needed to develop and implement criteria for the occurrence of meander-bend cutoffs. Future versions of the model could track the age of floodplain and terrace vegetation over time. As the model simulates the creation of point bars along the inside curves of meander bends, the model could also simulate the growth of vegetation on these point bars. Young vegetation could either be scoured by subsequent floods or grow to maturity and potentially protect the bank from future erosion. A future version of the model could also account for the increase in sediment supply caused by the erosion of terrace banks because they are higher in elevation than the floodplain surface.

REFERENCES

Dunne, T. and Leopold, L. B. (1978). "Water in environmental planning," W.H. Freeman and Company, New York, New York.

Leopold, L. B. (1994). A Vew of the River. Harvard University Press, Cambridge, Massachusetts.

Leopold, L. B., Wolman, M. G., and Miller, J. P. (1964). "Fluvial processes in geomorphology," W. H. Freeman and Company, San Francisco, California.

Piety, L. A., Bountry, J. A., Randle, T. J., and Lyon E. W. (2004). "Geomorphic assessment of the Hoh River, Washington, river miles 17 to 40 between Oxbow Canyon and Mount Tom Creek," U.S. Department of the Interior, Bureau of Reclamation, Denver, Colorado.

Randle, T.J. (2004). "Channel Migration Model For Meandering Rivers," A thesis submitted to the University of Colorado at Denver in partial fulfillment of the requirements for the degree of Masters of Science, Civil Engineering.

Thorne, C. R. (1992). "Inaugural lecture, River meanders: Nature's answer to the straight line," University of Nottingham, Department of Physical Geography, Nottingham, England.

Thorne, C. R., (2002). "Geomorphic analysis of large alluvial rivers," Geomorphology, 44, 203-219.

Yang, C. T. (1971). "On river meanders," Journal of Hydrology, 13, 231-253.

Yang, C. T. and Song, C. C. (1979). "Theory of minimum rate of energy dissipation," Journal of the Hydraulics Division, American Society of Civil Engineers, 105 (7), 769-784.